

Dynamical Complexity in Swarm Electron Density Time Series using Block Entropy

G. BALASIS¹, C. PAPADIMITRIOU^{1,2}, A. Z. BOUTSI^{1,3}, I. A. DAGLIS^{3,4,1}, O. GIANNAKIS¹, A. ANASTASIADIS¹, P. DE MICHELIS⁵ and G. CONSOLINI⁶

¹ *Institute for Astronomy, Astrophysics, Space Applications and Remote Sensing, National Observatory of Athens - Metaxa and Vas. Pavlou St., Penteli, 15236 Athens, Greece*

² *Space Applications & Research Consultancy, SPARC - 10551 Athens, Greece*

³ *Department of Physics, National & Kapodistrian University of Athens - Panepistimiopolis, Zografos, 15784 Athens, Greece*

⁴ *Hellenic Space Center - 15231 Athens, Greece*

⁵ *Istituto Nazionale di Geofisica e Vulcanologia - 00143 Rome, Italy*

⁶ *INAF-Istituto di Astrofisica e Planetologia Spaziali - 00133 Rome, Italy*

PACS 94.05.Sd – Space weather

PACS 94.30.Lr – Magnetic storms, substorms

PACS 89.75.-k – Complex systems

Abstract – Our goal in this study is to investigate the dynamical complexity of the electron density profiles in the topside ionosphere as measured by the Swarm mission, employing the use of symbolic information-theoretic techniques. We perform a Block entropy analysis for a time interval associated with the most intense magnetic storm of solar cycle 24, which occurred on 17 March 2015. We produce entropy maps for varying degrees of magnetospheric disturbance, resolving the different effects that the various geomagnetic activity levels have in the dynamics of the complex magnetosphere-ionosphere coupling system. Understanding the impact of these effects on the ionospheric plasma constitutes a crucial factor for the functionality of modern technological infrastructure operating around the Earth and, thus, human welfare.

Introduction. – Since the birth of modern Information Theory in the late 1940s [1], an ever expanding toolbox of methods and techniques for analyzing signals of natural or man-made origin has been applied to a wide variety of cases, in an attempt to capture different aspects of the dynamics of the underlying systems. The obvious interdisciplinary character of this approach offers refreshingly new insights into the analysis of data and can thus help illuminate aspects of the involved physical processes that have up to now remained untouched, but also poses significant challenges and issues, as the application of these methods cannot be thoughtlessly transferred from the field of Telecommunications (from which most of these ideas have emerged) to another scientific discipline.

The plasma density in the ionosphere is characterized by multi-scale irregularities that range from a few meters up to thousands of kilometers and which are related to atmospheric as well as magnetospheric conditions [2, 3]. These irregularities can have a wide range of implications,

affecting everything from communications between satellites and ground stations, the accuracy of Global Navigation Satellite Systems (GNSS) positioning as well as the propagation and/or reflection of radio signals [4, 5]. Due to all these reasons, the study of ionospheric turbulence and the mechanisms responsible for its generation, as well as its dynamics, is of great importance.

Geospace magnetic storms occur when the accumulated input power from the solar wind exceeds a certain threshold. They are extreme events producing a number of distinct physical effects in the near-Earth electromagnetic environment, including intensification of electric currents in space and on the ground, impressive aurora displays, and global magnetic disturbances on the Earth’s surface [6, 7].

Here, we propose to apply a Block entropy analysis based on symbolic dynamics techniques to the time series of the electron density measured on board the low-Earth orbit (LEO) satellites of European Space Agency’s (ESA) Swarm mission. We present a successful application of an

information theory approach at capturing the dynamical complexity of the in situ observations of ionospheric disturbances during the most intense magnetic storm of the last solar cycle, that occurred on 17 March 2015 with a minimum value of the Disturbance storm time (Dst) index of -223 nT. So far, only magnetic field data from the mission were analyzed using entropy measures and this was done only once and only very recently [8]. Therefore, the herein presented results shed light on aspects of the ionospheric response during an extreme episode of space weather from a quite different perspective, that of the electric field experiment on board the Swarm mission.

Method. – In the paper that marked the birth of Information Theory, Shannon [1] described all the mathematical properties that an Entropy-like measure (H) should possess and suggested a formula inspired by Ludwig Boltzmann’s [9] entropy definition for statistical physics, given by

$$H = - \sum p_i \cdot \log p_i \quad (1)$$

where p_i denotes the probability of the system being in a cell i of its phase space.

One of the many implications of this formalism is that it can be applied in any case where a probability can be defined and thus have a much wider range of applications. Especially in telecommunications, where a digital signal can be considered as a series of discrete states, the application of such a formula becomes simple and intuitive. Unfortunately, signals from natural systems rarely possess such a simple and discrete behavior; instead experimental observatories measure a small subset of continuous parameters, from which scientists attempt to draw conclusions on the state and dynamics of a system. Luckily, Shannon’s formula can still be applied to data series from such cases, by introducing a “digitization” step, where the values of the observed parameter are mapped to a discrete set of states, which can be considered as a different cell of the system’s phase space. Thus, the probabilities p_i can easily be computed from the frequency of occurrences of each such state. The manner in which this digitization is performed is critical for the type of information that will be captured from the signal and hence, for the analysis that will be performed. A series of thresholds, at equal distances from the minimum to the maximum values, can be easily employed for such a task, or alternatively a series of equally-spaced percentiles, although this second approach will automatically yield the maximum Shannon entropy value [10], as in this case all states will have equal probabilities. **Since this is essentially the same as constructing the histogram of the occurrence frequency of the various states, this type of analysis will be referred to as Histogram Entropy.**

Such a digitization of course maps many nearby values to the same state and thus results in a much more coarse view of the system and as such, less information. At the

same time though, this provides the opportunity to examine sequences of such states with much better statistics and not only focus on the instantaneous values, allowing more information on the dynamics and the temporal evolution of the system. In a sense, information on the precision of the observed parameter is being exchanged for information on properties such as its periodicities, symmetries or its chaotic nature in general [11]. Now the probabilities p_i will not refer to the probability of occurrence of any state, but to the combinations for all the possible successions of states and thus to the dynamics of the system [12].

The easiest example of this process is a binary digitization, where all values below a certain threshold are replaced by a symbol, e.g. 0, while all values above it with e.g. 1, thus creating a “symbolic sequence” of 0s and 1s, such as the 0110101100... This sequence can be read in terms of distinct consecutive blocks of length n , so for $n = 2$, one could read the series as the sequence of non-overlapping patterns 01, 10, 10, 11, 00 etc. in a parsing procedure that is called “lumping”, or alternatively read the series as a sequence of patterns that overlap by all but one element, hence producing the sequence 01, 11, 10, 01, 10, 01, 11 10, 00 and so on, in a procedure called “gliding”. Regardless of the approach used, in the end the number of occurrences of each possible n -block are counted and the probabilities of each calculated. Successively, they are used in the Shannon formula to produce the value of the Block Entropy $H(n)$ for block length n . Typically, gliding is more often used, as it produces more instances of blocks and thus a better statistics, while lumping is important for the detection of automaticity, in series that have been generated by finite automata or algorithmic processes [13]. $H(n)/n$ can be interpreted as the mean uncertainty per symbol [14, 15] and should converge for $n \rightarrow \infty$ to some stationary value if the underlying dynamics is deterministic. From a practical perspective however, one is often interested in quantifying the mean information gain when increasing the block length, measured by the conditional (or differential) block entropies:

$$h(n) = H(n + 1) - H(n) \quad \text{for } n \geq 1; h(0) = H(1) \quad (2)$$

For stationary and ergodic processes, the limit of $h(n)$ for $n \rightarrow \infty$ provides an estimator of the Kolmogorov-Sinai entropy or source entropy h of the dynamical system under study [16, 17]. Alternatively, one can compute $H(n)$ for various n values and if they exhibit a reasonably linear scaling vs n , estimate their gradient as another proxy for the limit of $h(n)$. This is what is being done in the present study.

Many real-world processes, like meteorological, hydrological, biological, medical, economic data etc., are intrinsically non-stationary since their probability density function (PDF) deforms when time evolves [18]. For these processes, the stationarity of the signal is often argued to be valid when considering small chunks of data span-

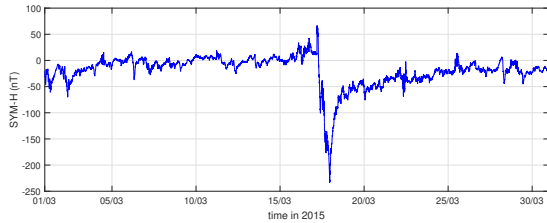


Fig. 1: SYM-H time series for March 2015.

ning short enough time range [19, 20], so that slow evolutions of higher order moments can be neglected. The non-stationary character of most space physics data sets requires methods that can appropriately treat such non-stationarities. In practice, the condition of stationarity for non-stationary signals can be satisfied by dividing the signal into blocks of short, pseudo-stationary segments [21]. In our case, the Swarm electron density time series were divided upon segments of 300 points, thus, satisfying the condition of non-stationarity for the purposes of the symbolic dynamics analysis. Furthermore, entropy measures constitute a versatile tool of analysis when dealing with non-stationary signals of dynamical systems like the signals originated from the magnetosphere, ionosphere or their coupling [22].

Data. — Launched on 22 November 2013, Swarm is the fourth in a series of pioneering Earth Explorer research missions and also ESA’s first constellation of satellites to advance our understanding of Earth’s magnetic field [23]. The Langmuir probes of the Electric Field Instrument (EFI) [24] on board the three satellites of Swarm provide electron density data in the form of time series, as the satellites fly through the topside ionosphere (Swarm A and C satellites fly side by side at an altitude of ~ 460 km while Swarm B satellite flies slightly above the lower pair of satellites at ~ 510 km). For this study, we have selected Level 1b 1 Hz electron density data for Swarm A (downloaded from the ESA ftp repository: <https://swarm-diss.eo.esa.int/>), covering a time window of one month, i.e., from 1 to 31 March 2015.

The hourly Dst index represents the average change of the horizontal component of the Earth’s magnetic field recorded at four mid-latitude magnetic observatories, which is caused by intensifications of the magnetospheric ring current that encircles the Earth and, thus, serves as a proxy of magnetic storm intensity. The SYMmetric disturbance field in H-component (SYM-H) index is essentially the 1-minute version of Dst, recorded at different sets of six mid-latitude observatories. On 17 March 2015 the strongest geomagnetic storm of solar cycle 24 took place. The SYM-H index captured that event, by reaching a minimum of -234 nT at the time, as is shown in Figure 1.

Results. — Attempting to capture the turbulent nature of the electron density series by means of entropic

measures is a very complex task that requires a lot of experimentation and fine-tuning of the parameters of the analysis, as the nature of the analysed signal is far different than the ones examined in previous studies [22, 25–30]. Special care should be taken, since the temporal and spatial scale of these features can be significantly smaller than those encountered in similar studies using e.g. the Dst index, where the scale of the phenomenon spans **hundreds to thousands** of kilometers and lasts for several days. Due to this, the analysis must be performed in significantly smaller time windows than the ones that have been employed in the previous studies, e.g. in the scale of a few minutes. With a cadence of 1 Hz, a time window of 5 minutes is enough to provide 300 measurements, i.e., data points, which can be used for processing. The full entropy analysis is being performed and then the window is moved forward in time by a 60-second step, which produces sequential windows that although overlap by 80% are able to capture even the very fast and small scale changes in the ion density series. Unfortunately, repeating ad-hoc the methods that were used in past in the case of the Dst Index or magnetic field data, is not enough to give meaningful results, as it can be shown in Figure 2. In this example, a couple of hours of electron density data from Swarm A, one of the two from the lower pair of satellites, during 15 March 2015 have been processed with various entropy methods, yielding discouraging results. The ion density series is shown with the blue line at the top panel of Figure 2 (as well as 3 and 4, which follow the same pattern), while the satellite’s position is indicated by the orange line, which depicts the Magnetic Latitude. In this case, both the histogram entropy, as well as the Block Entropy approach, with a binary symbolic representation (segmented at the window median) for both lumping and gliding parsing, all failed to capture any meaningful behavior. Similarly incomprehensible results were obtained for multi-symbol representations (up to 4 symbols) and for various other types of entropies (not shown here).

In order to fix these issues a new strategy was formulated performing the binary symbolic representation using as a threshold a constant value, that is not window-dependent. This approach provides a simple and intuitive way to distinguish between low latitudinal passes, where the ion density exhibits high values, and higher latitudes, where the ion densities are significantly lower. Thus, by using a high threshold, the binarization will work produce non-trivial sequences on the near-equatorial parts of the series, while a low threshold will focus on the low valued variations and hence on the middle and high latitudes. The result of the application of this method is reported in Figure 3. Although the histogram entropy fails to produce any meaningful result, the Block Entropies are capable of successfully capturing both the turbulent nature of the plasma by exhibiting near-zero values at windows where the satellite only measures smooth electron density profiles, and high entropy values at the times when the satellite flies through disturbances, as they are the ones

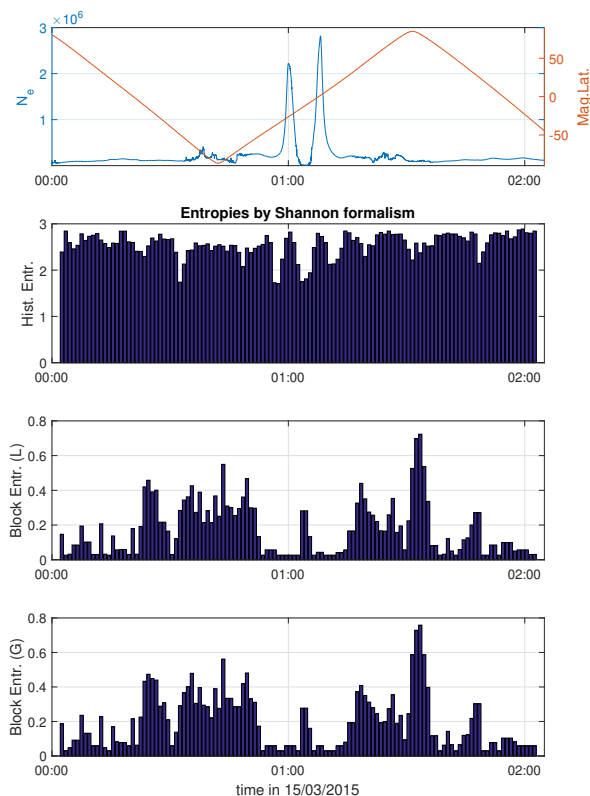


Fig. 2: Ad-hoc application of entropy methods on electron density time series from Swarm A.

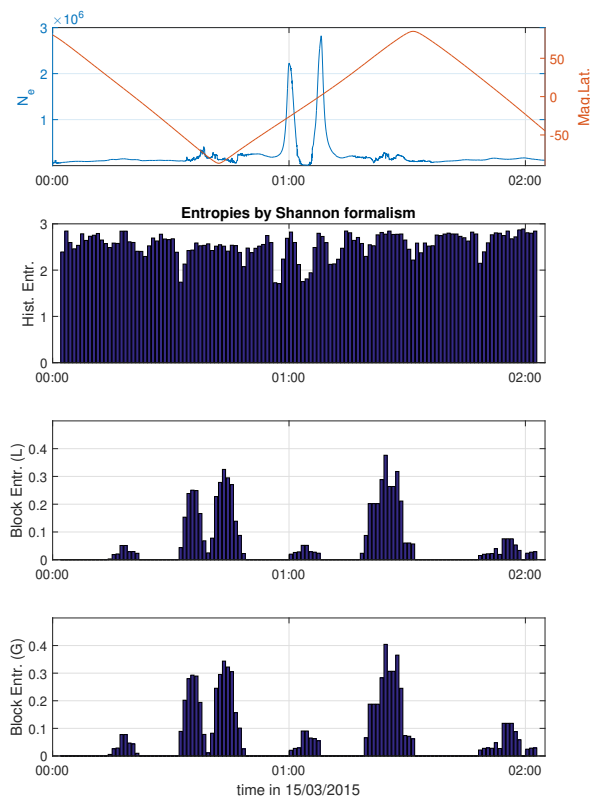


Fig. 3: Application of the new strategy of entropy methods on electron density time series from Swarm A (emphasizing high latitudes).

247 associated with the polar passes and the equator (high-
 248 lighted by the orange line that shows the satellite’s Mag-
 249 netic Latitude). Both Block Entropies are calculated on
 250 windows of binary symbolic sequences with length of 300
 251 points, which are moved forward in time by 60 points. For
 252 each such window, the Entropies are calculated for block
 253 lengths n from 1 to 4, producing the corresponding $H(n)$
 254 values. A simple least squares fitting then, produces the
 255 gradient of the $H(n)$ vs n line, which is the final entropy
 256 value. Since the maximum theoretical value for a binary
 257 representation is $\log(2)$, values are normalized by it to
 258 yield the final normalized entropy of each window.

259 As it is always happens in methods involving symbolic
 260 dynamics, or in general the digitization of a continuous
 261 signal to discrete “states”, the particular way with which
 262 this conversion takes place plays a critical role in capturing
 263 a specific portion of the information that is carried by the
 264 signal. In this case, the binarization has been performed
 265 by a constant threshold value and as it can be seen in Fig-
 266 ure 3 the entropies of the windows encountered at high
 267 latitudes exhibit higher values. The increase of thresh-
 268 old value can invert this behavior and produce a different
 269 image, with the low-latitude entropies taking the lead as
 270 shown in Figure 4. Thus, by changing the threshold of the
 271 binarization one can switch the emphasis from low latitude
 272 signals that are usually related to plasma bubbles [31] to
 273 high latitudes signals related to field aligned currents [32].

274 The analysis can be performed (for simplicity only for
 275 the gliding Block entropy) for the entire time span of the
 276 2015 St. Patrick’s storm. Since the satellite continuously
 277 moves in space, we save the position of the satellite for
 278 each entropy calculation (by considering the median value
 279 of the magnetic longitude and magnetic latitude for each
 280 window) and produce maps of the average entropy values
 281 of the electron density for the entire duration of the event,
 282 i.e. from 15 March to 23 March. Values are mapped on a
 283 36 by 30 grid, in magnetic coordinates, which amounts to
 284 a precision of 10 degrees in Magn. Long. and 6 degrees in
 285 Magn. Lat. Again, changing the threshold can produce
 286 two different versions of those maps, one emphasizing the
 287 low and another for the high latitudes. These results are
 288 shown in Figure 5. **At the lower panel of Figure 5,**
 289 **the largest red “blob” (presumably long lasting**
 290 **or extremely large during the storm) is centred**
 291 **around the equatorial region close to the South**
 292 **Atlantic Anomaly (SAA). The SSA is an unusually**
 293 **weak spot in the Earth’s magnetic field over South**
 294 **America and the southern Atlantic Ocean, allow-**
 295 **ing charged particles from the Sun to dip closer**
 296 **to the surface than normal. These particles may**
 297 **cause damage to satellites orbiting the Earth and**
 298 **crossing that area.**

299 Figure 6 shows entropy maps between pre-storm time (

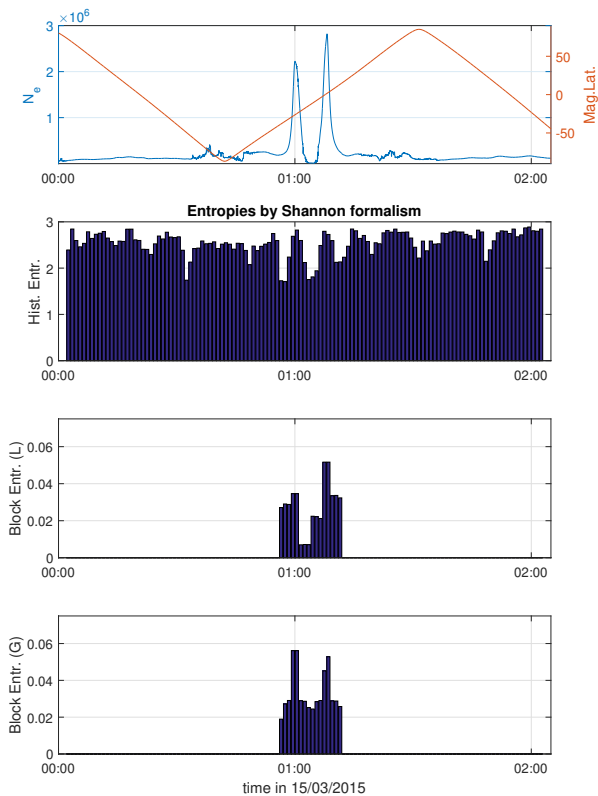


Fig. 4: Application of the new strategy of entropy methods on electron density time series from Swarm A (emphasizing low latitudes).

1-15 March 2015) and storm-time along with post-storm time (16-31 March 2015) for high-threshold (low latitudes).

Figure 7 shows entropy maps between pre-storm time (March 1 to 15 of 2015) and storm-time along with post-storm time (March 16 to 31 of 2015) for low-threshold (high latitudes).

In both Figures 6 and 7, we can see the drop in the entropy values as we move from the pre-storm period to the main phase and recovery phase of the storm (axes and color maps are identical in the two plots). Furthermore, the signature of the magnetic storm appears more prominent at low and mid latitudes, which are more closely related to the footprint of the magnetospheric ring current intensifications, than at high latitudes which are more seriously affected by magnetospheric substorms, presumably accompanying the intense magnetic storm.

A possible interpretation of the results presented in these maps could be the following: it is likely that the observed differences in the entropy values in periods before the storm against periods during and after the storm may be associated with the existence of different turbulence levels and not entirely with the presence of ionospheric plasma irregularities either at low and mid-latitudes [e.g. Equatorial Spread-F (ESF) signatures [33]] or at high latitudes [e.g. auroral plasma instabilities

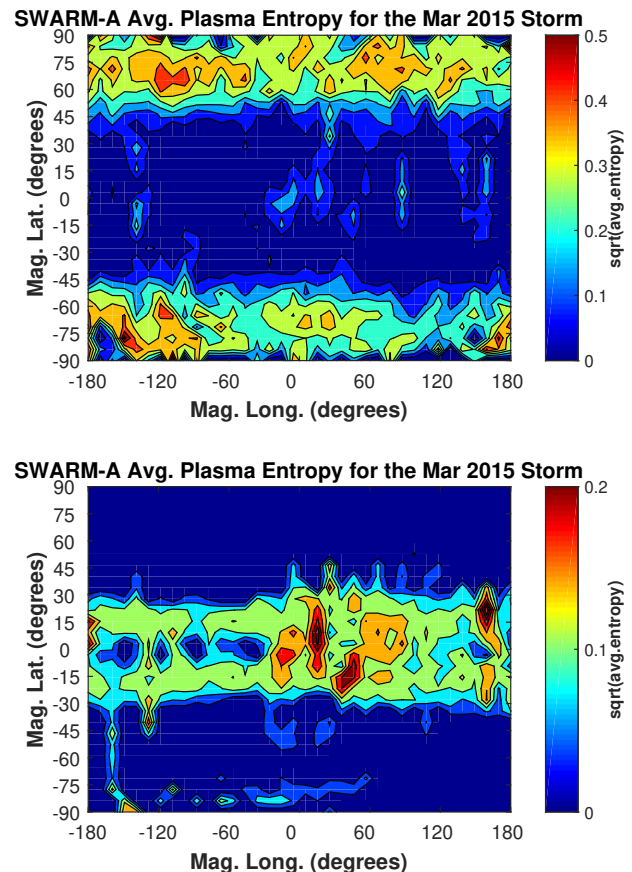


Fig. 5: Maps of the average entropy for Swarm A from 15 to 23 March 2015 [emphasizing (top) high and (bottom) low latitudes].

[34–36]]. We note that generally in the polar cap, the turbulence levels are much lower than those on auroral field lines [37]. Furthermore, the varying turbulence levels at high latitudes could also be attributed to wave-particle interactions triggered by the storm.

Conclusions. – In this study, we explore the use of Block entropy as a dynamics classifier for Swarm electron density observations, that were collected in the topside ionosphere over a period associated with the most intense magnetic storm of solar cycle 24. Similar information theory approaches have been previously used with success to investigate the dynamics of meteorological data [38].

We find that the entropy values of the Swarm electron density time series are higher in the time interval before the storm than during its main and recovery phase. Therefore, our findings clearly indicate a transition from a state with higher complexity or less order before the storm to a state with less complexity or more order during the storm and its recovery phase. These results are in agreement with earlier studies on the entropy analysis of geomagnetic activity indices [22, 26] and more recent studies on the entropy analysis of Swarm magnetic field data [8].

Information theory provides powerful tools for quanti-

349 fying the information content of complex systems like the
 350 complex magnetosphere-ionosphere coupling system. Our
 351 results advocate the capability of symbolic information-
 352 theoretic techniques to form a versatile diagnostic tool for
 353 a space weather related time series' dynamics.

354 The nature of the presently analyzed data from Swarm
 355 (electron density) is very different from the previously ana-
 356 lyzed data from the mission (magnetic field), following
 357 a different behavior and exhibiting different characteris-
 358 tics. Figures 2–4 emphasize these differences and the nec-
 359 cessity of taking a more sophisticated and computationally
 360 demanding approach in analyzing the electron density
 361 data using entropy measures than previously studies,
 362 when more straightforward entropy analyses were applied
 363 to magnetic field data. The fact that our present analy-
 364 sis led us to similar, qualitatively, information content
 365 for the Swarm electron density time series in compar-
 366 ison to the Swarm magnetic field time series is a step
 367 forward in the study of the dynamical complexity in the
 368 magnetosphere-ionosphere coupling system.

369 Furthermore, this science discovery based on informa-
 370 tion theory techniques could offer the possibility of an ad-
 371 ditional or alternative dataset (i.e., electron density) to the
 372 standard datasets (i.e., magnetic field) for applying future
 373 space weather prediction schemes. The latter is very use-
 374 ful, for instance, when considering the use of satellite data,
 375 which instrument failures are likely to unexpectedly occur
 376 due to various artificial and natural-environment reasons,
 377 since the electron density measurements can replace the
 378 magnetic field measurements as complexity indicators and
 379 vice versa.

380 The authors acknowledge financial support from Euro-
 381 pean Space Agency (ESA contract N. 4000125663/18/I-
 382 NB “EO 486 Science for Society Permanently Open Call
 383 for Proposals EOEP-5 BLOCK4” (INTENS)). C.P., G.B.,
 384 A.Z.B., I.A.D. and O.G. acknowledge additional finan-
 385 cial support from European Union’s Horizon 2020 re-
 386 search and innovation programme under grant agreement
 387 No 870437. This work was benefitted from discussions
 388 within the International Space Science Institute (ISSI)
 389 Team # 455 “Complex Systems Perspectives Pertaining
 390 to the Research of the Near-Earth Electromagnetic Envi-
 391 ronment”. This study makes use of data from the Swarm
 392 spacecraft mission, which is funded and managed by the
 393 European Space Agency (ESA). The Swarm data can be
 394 obtained from the ESA server at swarm-diss.esa.int.
 395 The Dst data are provided by the World Data Cen-
 396 ter for Geomagnetism, Kyoto ([http://wdc.kugi.kyoto-
 397 u.ac.jp/dst/dir/index.html](http://wdc.kugi.kyoto-u.ac.jp/dst/dir/index.html)).

398 REFERENCES

399 [1] SHANNON C. E., *Bell Syst. Tech. J.*, **27** (1948) 379-423.

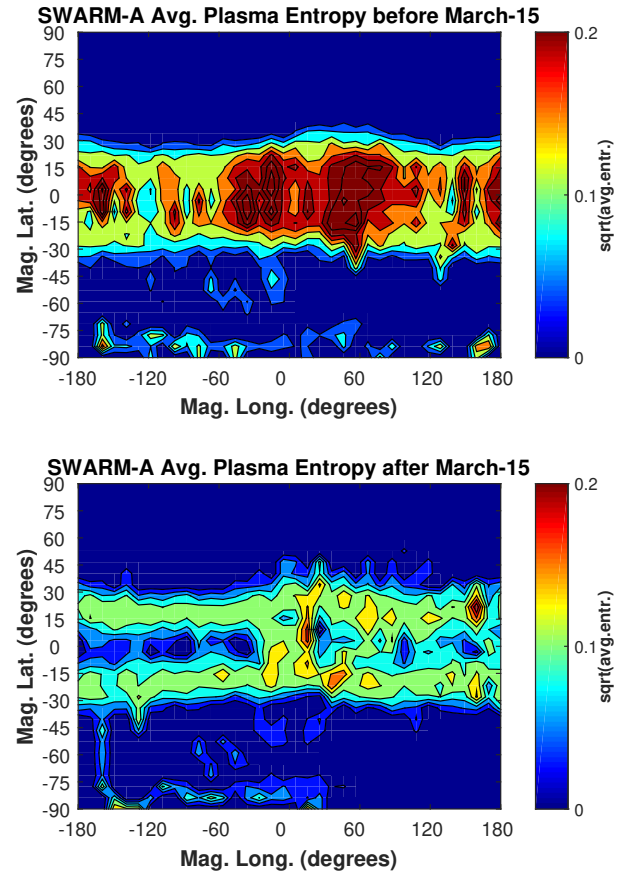


Fig. 6: Maps of average entropy between (top) pre-storm time (1-15 March 2015) and (bottom) storm-time as well as post-storm time (16-31 March 2015) for high-threshold (low latitudes).

- [2] KESKINEN M. J. and OSSAKOW S. L., *Radio Sci.*, **18(6)** (1983) 1077-1091. 400
 401
 [3] GIANNATTASIO F., DE MICHELIS P., CONSOLINI G., QUATTROCIOCCI V., COCO I. and TOZZI R., *Annals of Geophysics*, **62** (2019) . 402
 403
 [4] PRIKRYL P., JAYACHANDRAN P. T., MUSHINI S. C. and CHADWICK R., *Ann. Geophys.*, **29** (2011) 377-392. 405
 406
 [5] XIONG C., STOLLE C. and PARK J., *Ann. Geophys.*, **36** (2018) 679-693. 407
 408
 [6] DAGLIS I. A., BAKER D. N., GALPERIN Y., KAPPENMAN J. G. and LANZEROTTI L. J., *Eos Trans. AGU*, **82(48)** (2001) 585. 409
 410
 [7] DAGLIS I. A., KOZYRA J. U., KAMIDE Y., VASSILIADIS D., SHARMA A. S., LIEMOHN M. W., GONZALEZ W. D., TSURUTANI B. T. and LU G., *J. Geophys. Res.*, **108(A5)** (2003) d031208. 412
 413
 [8] PAPADIMITRIOU C., BALASIS G., BOUTSI A. Z., DAGLIS I. A., GIANNAKIS O., ANASTASIADIS A., DE MICHELIS P. and CONSOLINI G., *Entropy*, **22(5)** (2020) 574. 416
 417
 [9] TOLMAN R. C., *Clarendon, Oxford*, (1938) . 418
 419
 [10] KOTSIANTIS S. and KANELLOPOULOS D., *GESTS International Transactions on Computer Science and Engineering*, **32** (2006) 47-58. 420
 421
 [11] HAO B.-L., *Elementary Symbolic Dynamics and Chaos in Dissipative Systems*. (World Scientific: Singapore, Singa- 422
 423
 424

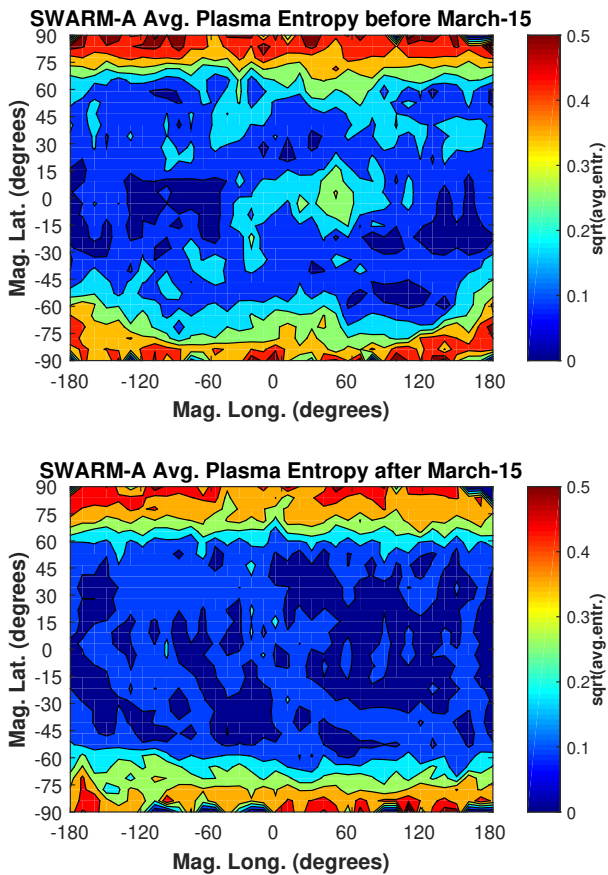


Fig. 7: Maps of average entropy between (top) pre-storm time (1-15 March 2015) and (bottom) storm-time as well as post-storm time (16-31 March 2015) for low-threshold (high latitudes).

425 pore) 1989.
 426 [12] KARAMANOS K. and NICOLIS G., *Chaos Solitons Fractals*,
 427 **10** (1999) 1135-1150.
 428 [13] KARAMANOS K., *AIP Conference Proceedings*, **573** (2001)
 429 278.
 430 [14] EBELING W. and NICOLIS G., *Chaos Soliton. Fract.*, **2**
 431 (1992) 635-650.
 432 [15] NICOLIS G. and GASPARD P., *Chaos Soliton. Fract.*, **4**
 433 (1994) 41-57.
 434 [16] KHINCHIN A.I., *Mathematical Foundations of Information*
 435 *Theory*. (Dover: New York, NY, USA) 1957.
 436 [17] McMILLAN B., *Ann. Math. Stat.*, **24** (1953) 196-219.
 437 [18] GRANERO-BELINCHÓN C., ROUX S. G. and GARNIER N.
 438 B., *Entropy*, **21** (2019) 1223.
 439 [19] FRISCH U., *Turbulence: The Legacy of A.N. Kolmogorov*
 440 (Cambridge University Press: Cambridge, UK) 1995.
 441 [20] IBE O., *Markov Processes for Stochastic Modeling*, 2nd ed.
 442 (Elsevier: London, UK) 2013, pp. 329-347-.
 443 [21] AKAY M., *Time Frequency and Wavelets in Biomedical*
 444 *Signal Processing Engineering* (Wiley-IEEE Press) 1997,
 445 p. 768.
 446 [22] BALASIS G., DAGLIS I. A., PAPADIMITRIOU C., KALIMERI
 447 M., ANASTASIADIS A. and EFTAXIAS K., *J. Geophys. Res.*,
 448 **114** (2009) A00D06.
 449 [23] FRIIS-CHRISTENSEN E., LÜHR H. and HULOT G., *Earth*

Planet Sp, **58** (2006) 351.
 450
 451 [24] KNUDSEN D. J., BURCHILL J. K., BUCHERT S. C., ERIKS-
 452 SON A. I., GILL R., WAHLUND J.-E., AHLÉN L., SMITH
 453 M. and MOFFAT B., *J. Geophys. Res. Space Phys.*, **122**
 454 (2017) 2655-2673.
 455 [25] BALASIS G., DAGLIS I., KAPIRIS P., MANDEA M., VAS-
 456 SILIADIS D. and EFTAXIAS K., *Ann. Geophys.*, **24** (2006)
 457 3557-3567.
 458 [26] BALASIS G., DAGLIS I. A., PAPADIMITRIOU C., KALIMERI
 459 M., ANASTASIADIS A. and EFTAXIAS K., *Geophys. Res.*
 460 *Lett.*, **35** (2008) L14102.
 461 [27] BALASIS G. and EFTAXIAS K., *Eur. Phys. J. Spec. Top.*,
 462 **174(1)** (2009) 219-225.
 463 [28] BALASIS G., DAGLIS I. A., ANASTASIADIS A., PAPADIM-
 464 ITRIOU C., MANDEA M. and EFTAXIAS K., *Physica A*,
 465 **390(2)** (2011) 341-346.
 466 [29] BALASIS G., DONNER R. V., POTIRAKIS S. M., RUNGE
 467 J., PAPADIMITRIOU C., DAGLIS I. A., EFTAXIAS K. and
 468 KURTHS J., *Entropy*, **15(11)** (2013) 4844-4888.
 469 [30] BALASIS G., POTIRAKIS S. M. and MANDEA M., *Front.*
 470 *Earth Sci.*, **4** (2016) 71.
 471 [31] PARK J., NOJA M., STOLLE C. and LÜHR H., *Earth*
 472 *Planet Sp*, **65** (2013) 13.
 473 [32] RITTER P., LÜHR H. and RAUBERG J., *Earth Planet Sp*,
 474 **65** (2013) 9.
 475 [33] BALASIS G., PAPADIMITRIOU C. and BOUTSI A. Z., *Phil.*
 476 *Trans. R. Soc. A.*, **377** (2019) .
 477 [34] SPICHER A., CAMERON T., GRONO E. M., YAKYMENKO
 478 K. N., BUCHERT S. C., CLAUSEN L. B. N., KNUDSEN D.
 479 J., McWILLIAMS K. A. and MOEN J. I., *Geophys. Res.*
 480 *Lett.*, **42** (2015) 201-206.
 481 [35] LIANG J., YANG B., DONOVAN E., BURCHILL J. and
 482 KNUDSEN D., *J. Geophys. Res.: Space Physics*, **122** (2017)
 483 8781-8807.
 484 [36] JIN Y., SPICHER A., XIONG C., CLAUSEN L. B. N., KER-
 485 VALISHVILI G., STOLLE C. and MILOCH W. J., *J. Geophys.*
 486 *Res.: Space Physics*, **124** (2019) 1262-1282.
 487 [37] KHAZANOV G. (Editor), *Space Weather Fundamentals*
 488 (CRC Press, Boca Raton) 2016.
 489 [38] LARSON J. W., BRIGGS P. R. and TOBIS M., *Procedia*
 490 *Computer Science*, **4** (2011) 1592-1601.